Published in final edited form as:
Dev Biol. 2009 March 1; 327(1): 48–61. doi:10.1016/j.ydbio.2008.11.028.

TGF-β3 and TNFα perturb blood-testis barrier (BTB) dynamics by accelerating the clathrin-mediated endocytosis of integral membrane proteins: A new concept of BTB regulation during spermatogenesis*

Weiliang Xia[+], **Elissa W. P. Wong**[+], **Dolores D. Mruk**, and **C. Yan Cheng**
Center for Biomedical Research, Population Council, 1230 York Avenue, New York, New York 10065

Abstract

In adult mammals such as rats, the blood-testis barrier (BTB) conferred by adjacent Sertoli cells in the seminiferous epithelium segregates post-meiotic germ cell development from the systemic circulation and is one of the tightest blood-tissue barriers. Yet it must "open" transiently at stage VIII of the epithelial cycle to accommodate the migration of preleptotene/leptotene spermatocytes. While this is a vital event of spermatogenesis, the mechanism(s) that regulates BTB dynamics is virtually unknown. Recent studies have suggested that transforming growth factor-β3 (TGF-β3) and tumor necrosis factor α (TNFα) secreted by Sertoli and germ cells into the microenvironment of the BTB are capable of inducing reversible BTB disruption *in vivo*, apparently by reducing the steady-state levels of occludin and zonula occludens-1 (ZO-1) at the BTB via the p38 mitogen activated protein (MAP) kinase signaling pathway. In this study, local administration of TGF-β3 (200 ng/testis) to the testis reversibly perturbed the BTB integrity *in vivo*. We next sought to delineate the mechanism by which these cytokines maintain the steady-state level of integral membrane proteins: occludin, junctional adhesion molecule-A (JAM-A) and N-cadherin at the BTB. Primary Sertoli cells cultured *in vitro* were shown to establish intact tight junctions and functional BTB within two days when assessed by transepithelial electrical resistance (TER) measurement across the cell epithelium. Sertoli cell integral membrane protein internalization at the BTB was assessed by biotinylation of cell surface proteins, to be followed by tracking the endocytosed/biotinylated proteins by using specific antibodies. Both TGF-β3 (3 ng/ml) and TNFα (10 ng/ml) were shown to significantly accelerate the kinetics of internalization of JAM-A, N-cadherin, and occludin *versus* controls. Treatment of cells with phenylarsine oxide (PAO) at 10 μM that blocks clathrin-mediated endocytosis was shown to inhibit the TGF-β3-induced protein internalization. This inhibition of TGF-β3-mediated protein endocytosis was further validated by silencing of clathrin. The specific effect of TGF-β3 on protein internalization was confirmed by RNAi using specific TGF-β receptor I (TβR1) siRNA duplexes. When TβR1 was knocked down, the TGF-β3-induced increase in the kinetics of JAM-A and occludin endocytosis was abolished, making them indistinguishable from controls, illustrating the specificity

*This work was supported in part by grants from the National Institutes of Health (NICHD, U01 HD045908; R03 HD051512; U54 HD029990 Project 5 to CYC), and the CONRAD Program (CICCR, C1G 01-72).

Address all correspondence to: C. Yan Cheng, Ph.D., The Mary M. Wohlford Laboratory for Male Contraceptive Research, Center for Biomedical Research, Population Council, 1230 York Avenue, New York, NY 10065, Fax: 212 327 8733, Email: Y-Cheng@popcbr.rockefeller.edu.
[+]These authors contribute equally to the completion of this work

of the TGF-β3 effects on protein endocytosis. In summary, this report demonstrates for the first time that BTB dynamics are regulated by TGF-β3 and TNFα via an enhancement of protein endocytosis at the BTB.

Keywords

testis; blood-testis barrier; spermatogenesis; cytokines; tight junction; ectoplasmic specialization; protein endocytosis

Introduction

Recent studies have shown that blood-testis barrier (BTB) dynamics during spermatogenesis are regulated, at least in part, by cytokines that determine the steady-state levels of integral membrane proteins at the BTB [for reviews, see (Lui and Cheng, 2007; Xia et al., 2005; Yan et al., 2007)]. For instance, it was shown that local administration of either TGF-β3 (Xia et al., 2006) or TNFα (Li et al., 2006) to testes of adult rats reversibly disrupted the BTB integrity when examined by dual-labeled immunofluorescence analysis using markers at the BTB, such as occludin, N-cadherin, JAM-A, and ZO-1. More important, local administration of TNFα to testes at concentration comparable to its endogenous level in the testis was shown to reversibly disrupt the BTB integrity. This was monitored by an *in vivo* functional assay by tracking the diffusion of a small fluorescent probe, such as fluorescein-5-isothiocyanate (FITC, Mr 389), from the systemic circulation to the adluminal compartment of the seminiferous epithelium following its administration at the jugular vein (Li et al., 2006). These results are consistent with recent observations in other epithelia, such as in small intestine and kidney, wherein cytokines are shown to be important regulators of tight junction (TJ) permeability barrier, such as in small intestine and kidney [for reviews, see (Walsh et al., 2000; Xia et al., 2005)]. These findings are important, since they illustrate that at the microenvironment of the BTB in the seminiferous epithelium, it is likely that cytokines, namely TNFα and TGF-β3 produced by Sertoli and/or germ cells (De et al., 1993; Skinner, 1993; Xia et al., 2006), contribute to the 'restructuring' and/or 'opening' of the BTB to facilitate the transit of preleptotene/leptotene spermatocytes across the BTB. This postulate is also supported by the observations that the expression of these cytokines was shown to be relatively high at or near the BTB during stage VIII of the epithelial cycle by immunohistochemistry (Lui et al., 2003a; Siu et al., 2003a; Xia et al., 2006). However, the mechanism by which cytokines induce a loss in the steady-state levels of integral membrane proteins at the BTB (e.g., occludin, JAM-A, N-cadherin) remains unknown.

Protein endocytosis plays a crucial role in regulating the steady-state levels of proteins at the cell junctions, which can be clathrin- or caveolin-dependent or via macropinocytosis [for reviews, see (Ivanov et al., 2005; Maxfield and McGraw, 2004)]. More importantly, it was postulated that the replacement of the apical ectoplasmic specialization [apical ES, a testis-specific actin-based atypical adherens junction (AJ) type] (Wong et al., 2008b) by apical tubulobulbar complex (apical TBC) to facilitate spermiation at stage VIII of the seminiferous epithelial cycle was mediated via protein internalization (Pelletier and Byers, 1992). Indeed, recent studies have supported this speculation wherein the adhesion domains of nectins 2 and 3 were found to be internalized as membrane vesicles near the TBC at spermiation (Guttman et al., 2004). In addition, recent studies have shown dynamin 2, a large GTPase known to be involved in protein endocytosis (McNiven et al., 2000; Sever et al., 2000) is structurally associated with integral membrane proteins at the BTB in rat testes (Lie et al., 2006). Furthermore, another isoform of dynamin, dynamin 3, was shown to be testis-specific (Kamitani et al., 2002). In light of these findings, we sought to examine if endocytosis is indeed taking place at the BTB of adult rat testes to regulate the steady-state levels of BTB- integral

membrane proteins to facilitate the transit of preleptotene/leptotene spermatocytes during the epithelial cycle of spermatogenesis. This is the subject of this report.

Materials and methods

Animals

Sprague-Dawley rats were purchased from Charles River Laboratories (Kingston, NY) and housed at the Rockefeller University Laboratory Animal Research Center with a 12 hr:12 hr light:dark cycle at 22 °C with access to rat chow and water *ad libitum*. The use of animals in this study was approved by the Rockefeller University Animal Care and Use Committee (Protocol Numbers: 03017 and 06018).

Primary Sertoli cell cultures

Primary Sertoli cell culture was prepared as previously described (Cheng et al., 1986; Xia et al., 2006). Freshly isolated Sertoli cells were cultured at 0.5×10^6 cells/cm^2 on Matrigel (BD Biosciences)-coated dishes as described (Xia et al., 2006) in serum-free Ham's F12 Nutrient Mixture and Dulbecco modified Eagle medium (F12/DMEM, 1:1, v/v, Sigma) containing HEPES (15 mM) and sodium bicarbonate (1.2 gm/L), supplemented with bovine insulin (10 μg/ml), human transferrin (5 μg/ml), epidermal growth factor (2.5 ng/ml), bacitracin (10 μg/ml), and gentamicin (20 μg/ml) as described (Mruk and Cheng, 1999). On the day of cell isolation, these cultures were designated as day 0. Matrigel was diluted 1:7 with F12/DMEM and dishes were coated 24 h prior to their use. These Sertoli cell cultures were incubated in a CO_2 incubator at 35 °C in a humidified atmosphere with 5% air/95% CO_2. About 36 hr thereafter, Sertoli cell cultures were subjected to a hypotonic treatment using 20 mM Tris, pH 7.4 at 22 °C for 2.5 min to lyse residual germ cells as described (Galdieri et al., 1981). Cultures were then washed twice in F12/DMEM. These Sertoli cells were contaminated with negligible germ cells when assessed by RT-PCR and/or immunoblotting using specific germ cell markers, such as c-kit receptor as described (Lee et al., 2004). Furthermore, by day 2 and thereafter these cultures were shown to form functional BTB when assessed by transepithelial electrical resistance (TER) measurement (Lui et al., 2001) across the Sertoli cell epithelium when cells were cultured on Matrigel-coated bicameral units. Additionally, functional BTB was detected as manifested by the presence of intact TJ and basal ES in these cultures on day 3 when examined by electron microscopy (Lee and Cheng, 2003; Siu et al., 2005). Indeed, these primary Sertoli cell cultures have been used by different laboratories including ours to study BTB function which mimic many of the functional and ultrastructural features of BTB *in vivo* (Byers et al., 1986; Chung et al., 2001; Janecki et al., 1991; Janecki et al., 1992). Media were replaced daily until these cultures were used on day 4 for the endocytosis assay to assess the effects of cytokines on the kinetics of endocytosis of integral membrane proteins at the BTB. Media collected on day 4 from selected cultures were used and served as Sertoli cell-conditioned media (SCCM).

Germ cell-conditioned medium (GCCM)

GCCM was prepared from freshly isolated total germ cells using a nonenzymatic mechanical method as detailed elsewhere (Aravindan et al., 1996). In short, total germ cells without elongating/elongated spermatids isolated from adult rat testes were cultured in F12/DMEM supplemented with sodium pyruvate (2 mM) and sodium lactate (6 mM) as described (Aravindan et al., 1996) at 35 °C in a humidified atmosphere with 5% CO2/95% air (v/v) for 14–16 hr. Thereafter, media were collected, centrifuged at 800 *g* for 20 min to remove cellular debris and the supernatant was collected and concentrated using a Millipore YM-10 membrane in an Amicon Model 8050 ultrafiltration unit.

In vivo BTB integrity assay

The *in vivo* BTB integrity assay was performed as earlier described (Li et al., 2006). In short, 200 ng recombinant TGF-β3 (R&D Systems, Minneapolis, MN) was administered locally to adult rat testis (~300 gm b.w.) on day 0 as described (Li et al., 2006). On day 2 and 14, rats (n=3 per treatment group for each time point) was anesthetized by ketamine HCl (60 mg/kg b.w., i.m.) with xylazine (10 mg/kg b.w., i.m.) as an analgesia. Rats without treatment/treated with vehicle (saline), or with $CdCl_2$ for 3 days at 3 mg/kg b.w. via i.p. were served as negative and positive controls, respectively. A small incision of about 0.5–1 cm above the jugular vein was opened and 200 μl of FITC (1 mg/ml) in PBS was administered into the jugular vein using a 28-gauge needle. The incision was then stitched, and rats were allowed to recover. About 60–90 min thereafter, rats were euthanized by CO_2 asphyxiation, and testes were immediately removed under aseptic conditions, and frozen in liquid nitrogen. Testes sections (about 8 μm) were obtained in a cryostat. All sections within an experimental set including controls and treatment groups were mounted with or without anti-fade reagent containing 4′,6′-diamidino-2-phenylindole (DAPI; Vector Laboratory, Burlingame, CA), and the green fluorescence for FITC was visualized in an Olympus BX40 fluorescent microscope. At least 100 tubules were randomly selected and acquired using an Olympus DP70 12.5 megapixel digital camera with the QCapture Software Suite (Version 2.56) (Quantitative Imaging Corp, Surrey, BC, Canada). Images were exported to TIFF format images. Distance of the FITC fluorescence that diffused away from the base of each seminiferous tubule (i.e., the relative location of the BTB near the basement membrane) (Df) in ~100 randomly selected tubules from two testes *versus* radius of the tubule (Rd) in treatment and control groups were computed. For oblique sections of seminiferous tubules, Rd was obtained by averaging the shortest and the longest distance from the basement membrane.

Endocytosis assay

Endocytosis assay was performed essentially as earlier described with minor modifications (Le et al., 1999; Morimoto et al., 2005). Briefly, Sertoli cells cultured at 0.5×10^6 cells/cm^2 on Matrigel-coated 6-well dishes for 4 days were washed twice with ice-cold PBS, incubated with 0.5 mg/ml Sulfo-NHS-SS-Biotin (Pierce) in PBS (10 mM sodium phosphate, 0.15M NaCl, pH 7.4 at 22 °C) containing 1 mM $CaCl_2$ and 0.7 mM $MgCl_2$ (PBS/CM) at 4 °C for 30 min to allow biotinylation of cell surface proteins. Excess Sulfo-NHS-SS-Biotin was quenched by 50 mM NH_4Cl in PBS/CM at 4°C for 15 min. Then cells were washed twice with ice-cold PBS and incubated with F12/DMEM with (test) or without (control) cytokines (TGF-β3 at 3 ng/ml and TNFα at 10 ng/ml), or with concentrated GCCM at 50 μg/ml, at 35 °C for various time points in a humidified atmosphere with 95% air and 5% CO_2 (v/v) to allow internalization of cell surface biotinylated proteins since endocytosis does not occur at 4 °C. At specified time points, cells were washed in cold PBS, incubated with a biotin stripping buffer [50 mM MESNA in 100 mM Tris/HCl (pH 8.6) containing 100 mM NaCl and 2.5 mM $CaCl_2$] at 4 °C for 30 min to remove any remaining biotin or non-endocytosed biotinylated proteins on the cell surface, and quenched with a quenching buffer [5 mg/ml iodoacetamide in PBS/CM] at 4 °C for 15 min. Thereafter, cells were washed twice with ice-cold PBS and lysed in an IP lysis buffer [10 mM Tris, pH 7.4 at 22 °C, containing 0.15 M NaCl, 2 mM PMSF, 1 mM EGTA, 1% NP-40 (v/v), 1 mM sodium orthovanadate, 1 μg/ml leupeptin, 1 μg/ml aprotinin and 10% glycerol (v/v)]. Equal amount of cell lysates (about 400 μg protein) between samples in an experiment were incubated with NeutrAvidin beads (Pierce) to pull down biotinylated proteins, washed three times in PBS, and biotinylated proteins were extracted in SDS sample buffer (Xia and Cheng, 2005). Proteins were resolved by SDS-PAGE, to be followed by immunoblot analysis using corresponding specific antibodies (see Table 1) to assess the kinetics of internalization of different integral membrane proteins.

Knockdown of TβRI and dynamins by RNAi using specific siRNA duplexes

Pre-designed siRNA duplexes targeting TβRI (Genbank Accession Number: NM_012775; Cat. # 16708-48442), dynamin 2 (Genbank Accession Number: NM_013199; Cat. # 16708-197996) and dynamin 3 (Genbank Accession Number: NM_138538; Cat. # 16708-193600) were purchased from Ambion (Austin, TX) and their sequences are listed in Table 2. In short, Sertoli cells at 0.5×10^6 cells/cm^2 were cultured for 2 days with negligible contamination of germ cells to allow the formation of an intact cell epithelium with functional TJ-barrier and the ultrastructures of BTB when examined by transepithelial electrical resistance (TER) and electron microscopy as described (Lui et al., 2003a;Siu et al., 2005). Thereafter, cells were transfected with specific siRNA duplex at 200 nM, using Oligofectamine (Invitrogen) for ~24 hr using protocols supplied by the vendor. Endocytosis assay was performed 2 days after transfection as described above and cultures were terminated at specified time point to assay changes in the kinetics of protein endocytosis. In selected experiments, cells that were transfected with specific siRNA duplex *versus* scrambled control siRNA duplex were harvested three days later for lysate preparation to confirm specific target protein knock down by immunoblot analysis.

Inhibition of protein endocytosis by using specific inhibitor and RNAi

Phenylarsine oxide (PAO) is an inhibitor of clathrin-dependent endocytic pathway (Ivanov et al., 2004). A recent report using specific inhibitors to clathrin (e.g., phenylarsine oxide, PAO) or caveolin (e.g., cholesterol oxidase, CO) have shown that protein endocytosis at the BTB using Sertoli cells cultured *in vitro* is likely mediated via the clathrin-dependent pathway (Yan et al., 2008). However, results derived from studies using specific inhibitors to study protein endocytosis should be cautiously interpreted (Ivanov, 2008); since PAO, besides blocking clathrin-mediated endocytosis, was shown to block macropinocytosis, phagocytosis (Frost et al., 1989; Massol et al., 1998), protein tyrosine phosphatase and Rho GTPase activity (Gerhard et al., 2003; Retta et al., 1996). PAO (Sigma-Aldrich) was used at 10 μM to examine its effects on TGF-β3-mediated enhanced endocytosis as described (Yan et al., 2008). Furthermore, to validate the earlier findings using inhibitors (Yan et al., 2008), we have re-examined the regulation of protein endocytosis at the BTB by cytokines (e.g., TGF-β3) using a more selective tool in which clathrin was knocked down by RNAi using specific clathrin siRNA *vs.* control scrambled duplexes. In short, Sertoli cells were isolated from 20-day-old rat testes (Day 0) as described above and plated at a density of 0.3×10^6 cells/cm^2 on Matrigel-coated dishes where ultrastructures of BTB, such as TJ and basal ES, were detected by electron microscopy as described (Siu et al., 2005). Two days after isolation (Day 2), cells were transfected with 100 nM siRNA (ON-TARGET plus set of 4 duplexes LQ-090659-01; Dharmacon) against rat clathrin heavy chain (Genbank Accession Number: NM_019299). On-target plus siControl non-targeting pool (D-001810-10; Dharmacon) was used as the corresponding control. 10 μl of TransIT-TKO transfection reagent (Mirus Bio) was used to transfect a total volume of 2 ml reaction mixture per well in 6-well culture dishes. Two days after transfection (Day 4), endocytosis assay was performed as described above. Biotinylated proteins were pulled down by NeutrAvidin beads (Pierce), washed four times with IP lysis buffer and extracted in SDS-sample buffer. Cell lysate was also harvested to assess the steady-state protein level of clathrin heavy chain after silencing. Under our experimental conditions, a ~50–60% reduction in clathrin protein level was observed. In preliminary experiments, a cell density of 0.5×10^6 cells/cm^2 was also used. However, at this higher cell density, Sertoli cells were required to be transfected twice in order to achieve acceptable knockdown when assessed by immunoblotting as previously described (Wong et al., 2008a), and endocytosis assay was performed 24 h after the second transfection (Day 8). Yet, endocytosis assays using Sertoli cells at higher density did not yield satisfactory result due to the diminished level of junction proteins on Day 8 of cells in culture (unpublished observations). Thus, the silencing condition was subsequently modified by using a lower cell density at 0.3×10^6 cells/cm^2 *vs.* 0.5×10^6 cells/cm^2, but BTB

ultrastructures were visible by electron microscopy, and functional TJ-barrier was still formed, and Sertoli cells were transfected only once with the corresponding siRNA or control duplexes on Day 2, with the endocytosis assay performing on Day 4 to examine the effects on the kinetics of protein endocytosis in the presence or absence of TGF-β3.

Dual-labeled immunofluorescence analysis and confocal microscopy

Sertoli cells were cultured on coverslips at 0.5–1 × 10^5 cells/cm^2 for dual-labeled immunofluorescence analysis. At specified time points following treatment *versus* controls, Sertoli cells were fixed in 4% paraformaldehyde (v/v) for 10 min, rinsed and treated with 10 mM glycine for 5 min to quench the aldehyde groups. Cells were permeabilized with 0.2% Triton X-100, rinsed and incubated with 10% normal goat serum in PBS for 15 min. For double-label immunofluorescence analysis, cells were incubated for 1 hr with the primary antibodies at appropriate dilutions (see Table 1), rinsed, and incubated for 1 hr with the relevant fluorescent secondary antibodies. Negative controls to assess staining specificity included incubation with normal IgG of the corresponding animal species of the primary antibodies or the omission of the primary antibodies. After extensive washing, coverslips were mounted on slides using Vectorshield mounting medium with DAPI (Vector Laboratory, Burlingame, CA). Images were examined and obtained by confocal microscopy and was performed at The Rockefeller University Bio-Imaging Resource Center with an inverted Zeiss LSM 510 Laser Scanning confocal microscope. Images were acquired using the Zeiss LSM 510 (v. 3.2) software and exported in TIFF format. Images were merged and analyzed using Adobe PhotoShop (Version 7.0).

To assess the effects of TGF-β3 on the ultrastructural changes at the BTB in adult rat testes by electron microscopy

Recombinant human TGF-β3 purchased from Calbiochem (Cat no. PF073) was resuspended and dissolved in 4 mM HCl containing 0.1% BSA (w/v). Just prior to its use, it was diluted in PBS to a concentration of 1 ng/μl. Adult rats (~300 gm b.w.) received 200 ng of recombinant TGF-β3 in a total volume of 200 μl per testis via intratesticular injection using a 28-gauge needle as described (Li et al., 2006) *versus* vehicle control with $n = 2$ rat per treatment or control group. Two days after TGF-β3 administration, rats were euthanized by CO_2 asphyxiation, testes were removed and processed for electron microscopy as described (Li et al., 2006; Yan and Cheng, 2006). Electron micrographs were obtained using a JEOL 100CXII Electron Microscope (Peabody, CA) at 80 kV at the Rockefeller University Bio-Imaging Resource Center.

Immunoblot analysis, immunoprecipitation and general methods

Immunoblotting and immunoprecipitation using the corresponding antibodies against different target proteins (see Table 1) were carried out as previously described (Xia and Cheng, 2005;Xia et al., 2006). Protein concentration in lysates was estimated by Coomassie blue-dye binding assay using BSA as a standard as described (Bradford, 1976). Proteins in GCCM were concentrated by ultrafiltration using an Amicon 8050 unit with YM-10 filters. Prior to their inclusion in the Sertoli cell cultures, GCCM was filtered via a 0.2-μm sterile filter unit and protein concentration was estimated and the desired concentration was appropriately adjusted by F12/DMEM under sterile conditions.

Statistical analysis

Each experiment was repeated at least three times using different batches of primary Sertoli cell cultures. Each time point in an experimental set contained triplicate cultures. Results of a treated sample group were compared to the corresponding control by ANOVA to be followed

by Tukey's Honest Significant Test or Dunnett's test using the GB-STAT Statistical Analysis Software package (Version 7.0) (Dynamic Microsystems Inc., Silver Spring, MD).

Results

Administration of TGF-β3 to rat testes in vivo reversibly disrupts the BTB integrity

As shown in Fig. 1, by local administration of recombinant human TGF-β3 (200 ng/testis) to adult rats (~300 gm b.w. at 100 days of age), the BTB integrity was shown to be disrupted by day 2 (Fig. 1A–B *vs.* D). This conclusion was reached since the BTB failed to restrict the FITC green fluorescence in the basal compartment of the seminiferous epithelium (see controls in Fig. 1A–B), resulting in the diffusion of FITC across the barrier. For instance, green fluorescence was detected in the seminiferous epithelium beyond the BTB in TGF-β3-treated rats, similar to rats treated with $CdCl_2$ except that it was not that extensive (Fig. 1D *vs.* C, and A–B). Cadmium is an environmental toxicant known to disrupt BTB integrity *irreversibly* in rats (Hew et al., 1993;Setchell and Waites, 1970;Wong et al., 2004). As shown in Fig. 1E, the TGF-β3-induced disruptive effect on the BTB integrity is transient, since by 14 days after the treatment, the BTB was shown to restrict the diffusion of the FITC across the barrier, similar to control rats (Fig. 1E *vs.* A–B). To further validate the effects of TGF-β3 on the BTB following its local administration into the testis, electron microscopy was performed as shown in Fig. 2. The BTB in adult rat testes is created by TJ (see the 'kisses' denoted by the black arrows) at the Sertoli-Sertoli cell interface which is also present side-by-side with the basal ES (Fig. 2A). Basal ES is typified by the presence of actin filament bundles (see black arrowheads) sandwiched between the endoplasmic reticulum (ER) and the plasma membrane (note: the two apposing Sertoli cell plasma membranes are denoted by the two opposing arrowheads) (see Fig. 2A), which co-exist with TJ. However, in rats treated with TGF-β3 for 2 days, distinguishable ultrastructural damages were visible at the Sertoli-Sertoli cell interface (see white arrowheads in Fig. 2B), and both TJ and basal ES were no longer detactable at the BTB in this rat testis (Fig. 2B *vs.* 2A).

It is likely that at stage VIII of the seminiferous epithelial cycle of spermatogenesis, TGF-β3 is secreted by Sertoli and/or germ cells into the BTB microenvironment near the basement membrane of the seminiferous epithelium, contributing to its 'restructuring' (and/or 'opening') to allow the transit of preleptotene/leptotene spermatocytes across the barrier. Thus, it is important to determine if similar level of TGF-β3 can be reached in the testis endogenously. Fig. 3A–F summarizes the results of a study using a solid-phase based immunoblot assay to assess the relative levels of TGF-β3 and TNFα in SCCM, GCCM *versus* testes (Fig. 2A, C) by plotting the relative amount of corresponding cytokine in these media/lysates against the recombinant proteins. As shown in Fig. 3B, D and summarized in Fig. 3E, F, it was estimated that SCCM, GCCM and testis lysates (in about 300 μg total protein) contained 7.5±0.7, 5.8 ±0.4, and 2.5±0.5 ng of TGF-β3 ($n = 3$) *versus* 1.5±0.2, 4.5±0.6, and 1.9±0.3 ng of TNFα ($n = 3$), respectively. This was equivalent to about 1.2±0.3 and 0.91±0.13 μg ($n = 3$) TGF-β3 and TNFα/testis, respectively, assuming the testis weight of an adult rat is ~1.6 gm, which was used to prepare testis lysates using a testis:IP buffer ratio of 1:3 (w:v), and protein concentration was obtained by Bradford reagent (Bradford, 1976). Thus, these results illustrate that the *in vivo* effects of TGF-β3 on the BTB integrity as shown in Fig. 1D and Fig. 2 are physiologically relevant since this concentration of TGF-β3 or a combination of cytokines (e.g., TGF-β3 and TNFα) can possibly be achieved at the BTB microenvironment at the site between Sertoli cells and preleptotene/leptotene spermatocytes, which transiently disrupts the BTB to facilitate the transit of preleptotene spermatocytes.

TGF-β3, TNFα and GCCM accelerate the internalization of integral membrane proteins at the BTB

Figure 4A summarizes the results of a representative set of experiments by monitoring the kinetics of endocytosis of several integral membrane proteins at the BTB: occludin, JAM-A, and N-cadherin. It was noted that the presence of TGF-β3 and TNFα enhanced the kinetics of endocytosis of biotinylated occludin, JAM-A and N-cadherin (Fig. 4A, B:a, b, c) from the Sertoli cell surface since significantly higher levels of these biotinylated integral membrane proteins were detected in the cytosol by 10 to 60 min (Fig. 4A, B). GCCM at 50 μg/ml was also effective in accelerating the internalization of biotinylated cell surface integral membrane proteins (Fig. 4A, B) possibly due to the presence of cytokines, in particular TNFα, in GCCM (see Fig. 3). However, the steady-state levels of the three BTB integral membrane proteins: occludin, JAM-A, and N-cadherin, in lysates from these cultures subjected to biotinylation and endocytosis assay with or without treatment with TGF-β3, TNF-α or GCCM *vs.* controls did not alter considerably (Fig. 4A, bottom four panels). These results were further verified by fluorescent microscopy as shown in Fig. 5A, B. For instance, in control Sertoli cell cultures without treatment with any cytokine, biotinylated proteins mostly localized at the cell surface (green fluorescence, FITC-streptavidin that bound to biotin), co-localizing with either occludin (red fluorescence) (Fig. 5A:a, b, c) or JAM-A (red fluorescence) (Fig. 5B:a, b, c) (see white arrowheads). By 30 min, cell surface biotinylated occludin (Fig. 5A:d, e, f) and JAM-A (Fig. 5B: d, e, f) were internalized (see white arrowheads); however, more occludin (Fig. 5A: h, i) and JAM-A (Fig. 5B: h, i) in the TGF-β3 treated Sertoli cell cultures were found to be internalized, moving away from the cell-cell interface (Fig. 5A: g, h, i and Fig. 5B: g, h, i). Furthermore, 3-dimensional projections of selected images (f & i) were reconstructed from a series of confocal images (z-stack) using the Imaris software (see f' and i' corresponding to f and i in Panels A and B), from which the protein internalization was better visualized. It is obvious that based on this analysis, TGF-β3 was capable of disrupting JAM-A- & occludin-based TJ fibrils via enhanced endocytosis, consistent with results shown in Fig. 4A, B.

Effects of silencing of Tβ R1 and dynamins by RNAi on protein endocytosis at the BTB

To further validate the effects of TGF-β3 and to assess the role of dynamins in mediating protein endocytosis at the BTB, RNAi was used to knock down TβR1, dynamin 2 or dynamins 2 and 3. Treatment of Sertoli cells with either TβR1- or dynamin 2-specific siRNA duplex *versus* scrambled siRNA duplex (controls) was shown to specifically knockdown the steady-state level of the corresponding protein by ~50–60% without affecting the other protein, illustrating the specificity of this technique (Fig. 6A, B). Interestingly, partial knockdown of dynamin 2 in Sertoli cells by RNAi had no apparent effects on the endocytosis of JAM-A at the BTB (Fig. 6C, D). However, treatment of Sertoli cells with TβR1 siRNA duplex was shown to abolish the TGF-β3-induced acceleration of endocytosis of biotinylated JAM-A, but not TNFα-induced acceleration of protein endocytosis (Fig. 6E, F). Interestingly, while RNAi of dynamin 2 alone had no apparent effects on protein endocytosis (Fig. 6C, D), when both dynamins 2 and 3 were knocked down, protein internalization was disrupted significantly at the 60-min time point (Fig. 6G, H *vs.* C, D). Furthermore, silencing of dynamins 2 and 3 also disrupted the TGF-β3- and TNFα-induced acceleration of protein endocytosis at both 10- and 60-min (Fig. 6G, H).

TGF-β3-induced acceleration of protein internalization is mediated via the clathrin-dependent pathway—Phenylarsine oxide (PAO) is a known inhibitor of clathrin-dependent pathway of protein endocytosis (Ivanov et al., 2004). The presence of PAO in the Sertoli cell cultures at 10 μM alone was shown to block the endogenous internalization of occludin, JAM-A and N-cadherin (Fig. 7A, B), illustrating the endocytosis of these proteins at the BTB is likely mediated via the clathrin-dependent pathway. The presence of PAO also abolished the TGF-β3-induced acceleration of protein endocytosis (Fig. 7A, B). However,

PAO is known to block macropinocytosis, phagocytosis (Frost et al., 1989; Massol et al., 1998), protein tyrosine phosphatase and Rho GTPase activity (Gerhard et al., 2003; Retta et al., 1996). To further validate these data, a more specific approach by targeting clathrin was used. Specific siRNA duplex was used to knock down clathrin protein level by ~50–60% in primary Sertoli cells with established BTB as shown in Fig. 8A, B. Consistent with results obtained by using inhibitor such as PAO (see Fig. 7), the knockdown of clathrin by RNAi significantly blocked the accelerated endocytosis of JAM-A induced by TGF-β3 (Fig. 8C, D). While the use of RNAi to silence clathrin failed to block protein endocytosis as effective as an inhibitor (Fig. 8 *vs*. Fig. 7) since we only managed to knock-down ~60% of the clathrin steady-state protein level in these primary Sertoli cell cultures and some JAM-A continued to be endocytosed in the transfected Sertoli cells (Fig. 8C), it is obvious that the knockdown of clathrin blocked the TGF-β3-mediated acceleration of JAM-A endocytosis (Fig. 8C, D). Furthermore, the knockdown of clathrin by RNAi also considerably reduced BTB integral membrane protein (e.g., JAM-A) endocytosis (see Fig. 8C, top panel *versus* Fig. 4A, second panel) due to the remaining clathrin available to the Sertoli cells in the system. It is also noted that the steady-state protein level of JAM-A in the cell lysates from cultures subjected to clathrin knockdown with or without treatment with TGF-β3 did not alter significantly (Fig. 8C, lower panel, and Fig. 8E).

Discussion

For more than three decades since the detailed morphological study illustrating the migration of preleptotene and leptotene spermatocytes across the BTB that takes place at stages VIII–IX of the seminiferous epithelial cycle of spermatogenesis in adult rats (Russell, 1977), the biochemical mechanism(s) that regulates this event, however, remains virtually unknown. Even though recent studies have shown that cytokines, such as TGF-β3 and TNFα, regulate the steady-state levels of integral membrane proteins at the BTB (e.g., occludin, ZO-1, claudins) (Hellani et al., 2000; Lui et al., 2001; Lui et al., 2003b; Siu et al., 2003a; Wong et al., 2004; Xia and Cheng, 2005), thereby determining the status of the BTB integrity plausibly via their effects on the transcriptional regulation of specific target genes such as claudins [for a review, see (Lui and Cheng, 2007)], the precise mechanism that is used by the testis involving cytokines to maintain the optimal integral membrane protein levels at the BTB remains obscure. Recent findings based on studies from different epithelia have shown that protein endocytosis is a novel mechanism utilized by a cell epithelium to rapidly alter cell junction dynamics, necessary to facilitate cell movement during embryogenesis, differentiation, and development (Ivanov et al., 2004; Le et al., 1999; Morimoto et al., 2005), it is of interest to determine if the transit of preleptotene/leptotene spermatocytes across the BTB employs similar mechanism involving cytokines, in particular Sertoli and germ cells are known to produce different cytokines in the seminiferous epithelium at relative high concentrations [for reviews, see (Cheng and Mruk, 2002; Mruk and Cheng, 2004; Skinner, 1993)].

In this report, it was shown that TGF-β3 when administered locally to the testis at 0.2 μg/testis, which is the concentration well within the endogenous range of TGF-β3 in normal testes, at 1.2±0.3 μg/testis when assessed by a solid-phase immunoblot-based assay, TGF-β3 was shown to reversibly disrupt the BTB integrity when assessed by a functional *in vivo* assay. These findings, coupled with the recent studies in which local administration of TNFα was also capable of inducing reversible BTB integrity disruption *in vivo* (Li et al., 2006), thus suggest that cytokines produced by Sertoli and germ cells locally [for reviews, see (Mruk and Cheng, 2004; Siu and Cheng, 2004; Skinner, 1993)] at the BTB microenvironment can regulate BTB dynamics possibly by regulating the steady-state levels and/or enhancing endocytosis of integral membrane proteins at the BTB (e.g., occludin, JAM-A and N-cadherin), causing a transient dissolution of the TJ-fibrils at the site, thus facilitating the transit of preleptotene/leptotene spermatocytes across the BTB. As shown in this report, the effects of TGF-β3 that

enhance protein endocytosis appear to be specific since a partial knock-down of TβRI, the specific receptor for TGF-β, rendered the Sertoli cell cultures with functional BTB incapable of responding to TGF-β3 treatment to accelerate protein endocytosis. The schematic drawing depicted in Fig. 9 illustrating the hypothesis that cytokines (e.g., TGF-β3 and TNFα) contributed by Sertoli and germ cells to the microenvironment at BTB to facilitate spermatocytes in transit is further supported by the findings that TGF-β3 expression at the BTB is stage-specific and its localization at the site of the BTB in the seminiferous epithelium of adult rat testes is relatively high at stages VII–VIII of the epithelial cycle when examined by immunohistochemistry technique (Lui et al., 2003a; Xia et al., 2006). Furthermore, TβR1 was also detected at the BTB by immunohistochemistry at these stages (Xia et al., 2006). The present report thus strengthens the notion that as a preleptotene/leptotene spermatocyte from the basal compartment begins its transit crossing the BTB to enter the adluminal compartment to continue its further development, cytokines are released near its apical region to enhance endocytosis, thereby inducing transient restructuring of the BTB to facilitate cell movement as illustrated in Fig. 9. However, it remains to be determined if the TGF-β3-induced germ cell loss from the seminiferous epithelium as recently reported (Xia et al., 2006) is also mediated by accelerated endocytosis of proteins at the apical ES and/or desmosome-like junctions at the Sertoli-elongating/elongated spermatid and Sertoli-spermatocyte interface. Thus similar investigation should be expanded to the use of Sertoli-germ cell cocultures or similar systems in future studies.

It is of interest to note that by silencing dynamin 2 or both dynamins 2 and 3 via the use of specific dynamin duplexes, it failed to disrupt endocytosis of JAM-A at the BTB in the absence of cytokines. Yet the silencing of dynamins 2 and 3 can effectively block the TGF-β3- and TNFα-induced enhanced endocytosis of integral membrane proteins at the BTB. It seems that while these large GTPases are used by other epithelia to regulate protein endocytosis (McNiven et al., 2000), they are not involved in protein endocytosis under normal conditions. However, a surge of cytokines at the BTB microenvironment may have recruited or activated other adaptors (or kinases, phosphatases) which, in turn, render the physiological involvement of dynamins in this event to accelerate protein endocytosis. This postulate is supported by recent findings that a disruption of germ cell adhesion in the seminiferous epithelium is associated with a transient increase in the binding of dynamin 2 with β-catenin, pulling β-catenin away from the cadherins, thereby destabilizing Sertoli-germ cell adhesion (Lie et al., 2006). This possibility is also supported by recent findings that FAK and Src, both are non-receptor protein tyrosine kinases, are prominently present at the BTB as visualized by immunohistochemistry and fluorescent microscopy (Lee and Cheng, 2005; Siu et al., 2003b). These kinases can thus activate and recruit dynamins to the BTB site to accelerate protein endocytosis to facilitate the transit of preleptotene/leptotene spermatocytes.

In epithelia, protein endocytosis is mediated via either clathrin-dependent, caveolin-dependent, or clathrin and caveolin-independent (e.g., macropinocytosis) mechanism [for reviews, see (Ivanov et al., 2005; Maxfield and McGraw, 2004)]. A recent report using specific inhibitors to clathrin (e.g., PAO) or caveolin (e.g., cholesterol oxidase, CO) have shown that protein endocytosis at the BTB using Sertoli cells cultured *in vitro* is likely mediated via the clathrin-dependent pathway (Yan et al., 2008). However, many of these classical inhibitors employed to study protein endocytosis are not specific (Ivanov, 2008). For instance, PAO, besides blocking clathrin-mediated endocytosis, also blocked macropinocytosis and phagocytosis, protein tyrosine phosphatase and Rho GTPase activity (Frost et al., 1989; Gerhard et al., 2003; Massol et al., 1998; Retta et al., 1996). In this study, we have used a more specific approach by RNAi using specific siRNA duplexes to knock down clathrin *versus* scrambled control siRNA duplexes. Using primary Sertoli cell cultures with established BTB including the functional TJ-permeability barrier *in vitro*, we managed to knock down ~60% of the clathrin protein in these Sertoli cells. While Sertoli cells continued to endocytose BTB proteins (e.g.,

JAM-A) at a considerably level following the partial knockdown of clathrin, TGF-β3 was no longer capable of enhancing JAM-A endocytosis because of a lack of clathrin in the Sertoli cell epithelium. These findings thus support a recent report (Yan et al., 2008) and results reported herein using inhibitors, illustrating protein endocytosis, in particular TGF-β3-induced accelerated endocytosis, that occurs at the BTB is mediated by a clathrin-dependent mechanism.

Present studies in the field have shown that endocytosed proteins in epithelial cells can either (i) be recycled back to the cell surface via recycling endosomes or undergo de-ubiquitination, or (ii) be recruited to late endosome to be targeted to lysosomes or undergo ubiquitination and targeted to proteasomes for intracellular degradation [for reviews, see (Bright et al., 2005; Katzmann et al., 2002; Lui and Cheng, 2007; Maxfield and McGraw, 2004; Piper and Luzio, 2007). It remains to be determined if the TGF-β3- and TNFα-induced endocytosed proteins would be targeted to lysosomes or proteasomes for intracellular degradation, *or* the percentage of endocytosed proteins being targeted for intracellular degradation via lysosomes and/or proteasomes *versus* recycling are differentially regulated, thereby reducing the steady-state levels of integral membrane proteins at the BTB, destabilizing the barrier function at the BTB to facilitate preleptotene/leptotene spermatocyte migration during spermatogenesis. However, using Sertoli cells with established BTB, TGF-β2 and testosterone were shown to enhanced protein endocytosis at the BTB, such as occludin (Yan et al., 2008). But TGF-β2 apparently promoted endocytosed occludin to late endosomes for its intracellular degradation via an increase in association with Rab 9 (a late endosome marker); whereas testosterone stimulated protein recycling (Yan et al., 2008), possibly relocating integral membrane proteins at the BTB near the apical region of a preleptotene spermatocyte in transit to its basal region. This possibility is consistent with the recent findings that testosterone is important to BTB function (Meng et al., 2005; Wang et al., 2006). The present report not only confirms some of these earlier findings, it has unequivocally demonstrated that protein endocytosis at the BTB, such as JAM-A, is mediated via a clathrin-dependent mechanism. Also, besides TGF-β2, TNFα and TGF-β3 can also regulate BTB restructuring via protein endocytosis. In this context, it is of interest to note that the effects of TGF-β3 on the endocytosis of some BTB integral membrane proteins, such as JAM-A, are more potent than TGF-β2 (Yan et al., 2008). This is not entirely unprecedented, since all TGF-βs and their related family members (such as activins, inhibins, bone morphogenetic protein) exert their biological effects via interactions with one of the three TGF-β binding proteins (or receptors) but with different affinities, which, in turn, determines the different biological potencies of different ligands (i.e., TGF-βs or their members) [for reviews, see (Bovd et al., 1990; Massague, 2008)]. These findings also suggest that different cytokines may be expressed temporally and/or spatially at the BTB microenvironment during the epithelial cycle at the time preleptotene spermatocytes are in transit at the BTB by regulating the relocation of proteins at the Sertoli-Sertoli cell interface, such as from the apical region of a migrating spermatocyte to its basal region, via transcytosis. Nonetheless, this possibility must be vigorously investigated in future studies.

It is noted that in the endocytosis assays, there were variations in the recovery of endocytosed biotinylated proteins *versus* total biotinylated proteins between experiments. This is possibly due to the multi-step processing of samples in these assays: (i) lysates preparation, (ii) the pull-down of biotinylated total proteins by avidin-based beads, (iii) SDS-PAGE, to be followed by (iv) immunoblotting using corresponding antibodies to visualize a specific target protein in the cytosol over an experimental period to detect the endocytosed and biotinylated protein. Indeed, we had minimized intra-experimental variations by processing all samples within an experimental set simultaneously so that any loss of biotinylated proteins would occur uniformly across the samples in a given experiment. Yet, given the number of steps that were involved to process these samples biochemically, it is difficult to conclude that the amount of endocytosed junctional proteins (e.g., JAM-A) is small (such as those shown in Fig. 6E)

because of the potential loss of samples during their processing. However, for data reported in Fig. 5B (see g–i *versus* a–f), these are the 'real-time' JAM-A at the cell-cell interface following TGF-β3 treatment at 30-min, but these results could not yield the time-dependent changes in endocytosis as those depicted in Fig. 6E nor be able to yield semi-quantitative information. But this technique is helpful to assess any changes in protein distribution (such as redistribution or mislocalization) in the Sertoli cells. Again, it is difficult to conclude that there was any loss of JAM-A at the cell-cell interface based on fluorescent staining by confocal microscopy except to conclude that more JAM-A was internalized following treatment with TGF-β3. These observations also expose the limitations of these two powerful and widely used techniques in the field, namely the biochemical-based endocytosis assay and the dual-labeled immunofluorescence analysis by confocal microscopy.

In summary, based on the results reported herein, we have provided a working model possibly used by the testis to regulate the transient 'opening' and 'closing' of the BTB during spermatogenesis involving cytokines and protein endocytosis as depicted in Figure 9. This model will now provide a basis for investigators in the field to design functional experiments to examine the intriguing regulation of junction dynamics at the BTB.

Acknowledgments

The authors thank Dr. Alison North at The Rockefeller University Bio-Imaging Resource Center for her helpful discussion on the use of confocal microscopy. We are also grateful for the excellent technical assistance of Ms. Eleana Sphicas at The Rockefeller University Bio-Imaging Resource Center for performing electron microscopy.

References

Aravindan GR, Pineau C, Bardin CW, Cheng CY. Ability of trypsin in mimicking germ cell factors that affect Sertoli cell secretory function. J Cell Physiol 1996;168:123–133. [PubMed: 8647906]

Bovd FT, Cheifetz S, Andres J, Laiho M, Massague J. Transforming growth factor-β receptors and binding proteoglycans. J Cell Sci (Suppl) 1990;13:131–138. [PubMed: 1964683]

Bradford M. A rapid and sensitive method for the quantitation of microgram quantities of protein utilizing the principle of protein-dye binding. Anal Biochem 1976;72:248–254. [PubMed: 942051]

Bright NA, Gratian MJ, Luzio JP. Endocytic delivery to lysosomes mediated by concurrent fusion and kissing events in living cells. Curr Biol 2005;15:360–365. [PubMed: 15723798]

Byers S, Hadley MA, Djakiew D, Dym M. Growth and characterization of epididymal epithelial cells and Sertoli cells in dual environment culture chambers. J Androl 1986;7:59–68. [PubMed: 3944021]

Cheng CY, Mather JP, Byer AL, Bardin CW. Identification of hormonally responsive proteins in primary Sertoli cell culture medium by anion-exchange high performance liquid chromatography. Endocrinology 1986;118:480–488. [PubMed: 3080306]

Cheng CY, Mruk DD. Cell junction dynamics in the testis: Sertoli-germ cell interactions and male contraceptive development. Physiol Rev 2002;82:825–874. [PubMed: 12270945]

Chung NP, Mruk DD, Mo MY, Lee WM, Cheng CY. A 22-amino acid synthetic peptide corresponding to the second extracellular loop of rat occludin perturbs the blood-testis barrier and disrupts spermatogenesis reversibly *in vivo*. Biol Reprod 2001;65:1340–1351. [PubMed: 11673248]

De S, Chen H, Pace J, Hunt J, Terranova P, Enders G. Expression of tumor necrosis factor-α in mouse spermatogenic cells. Endocrinology 1993;133:389–396. [PubMed: 8319585]

Frost SC, Lane MD, Gibbs EM. Effect of phenylarsine oxide on fluid phase endocytosis: Further evidence for activation of the glucose transporter. J Cell Physiol 1989;141:467–474. [PubMed: 2687296]

Galdieri M, Ziparo E, Palombi F, Russo M, Stefanini M. Pure Sertoli cell cultures: a new model for the study of somatic-germ cell interactions. J Androl 1981;5:249–259.

Gerhard R, John H, Aktories K, Just I. Thiol-modifying phenylarsine oxide inhibits guanine nucleotide binding of Rho but not of Rac GTPases. Mol Pharmacol 2003;63:1349–1355. [PubMed: 12761345]

Guttman JA, Takai Y, Vogel AW. Evidence that tubulobulbar complexes in the seminiferous epithelium are involved with internalization of adhesion junctions. Biol Reprod 2004;71:548–559. [PubMed: 15084482]

Hellani A, Ji J, Mauduit C, Deschildre C, Tabone E, Benahmed M. Developmental and hormonal regulation of the expression of oligodendrocyte-specific protein/claudin 11 in mouse testis. Endocrinology 2000;141:3012–3019. [PubMed: 10919290]

Hew K, Heath G, Jiwa A, Welsh M. Cadmium *in vivo* causes disruption of tight junction-associated microfilaments in rat Sertoli cells. Biol Reprod 1993;49:840–849. [PubMed: 8218650]

Ivanov AI. Pharmacological inhibition of endocytic pathways: is it specific enough to be useful? Methods Mol Biol 2008;440:15–33. [PubMed: 18369934]

Ivanov AI, Nusrat A, Parkos CA. Endocytosis of epithelial apical junction proteins by a clathrin-mediated pathway into a unique storage compartment. Mol Biol Cell 2004;15:176–188. [PubMed: 14528017]

Ivanov AI, Nusrat A, Parkos CA. Endocytosis of the apical junctional complex: mechanisms and possible roles in regulation of epithelial barriers. BioEssays 2005;27:356–365. [PubMed: 15770686]

Janecki A, Jakubowiak A, Steinberger A. Effects of cyclic AMP and phorbol ester on transepithelial electrical resistance of Sertoli cell monolayers in two-compartment culture. Mol Cell Endocrinol 1991;82:61–69. [PubMed: 1722179]

Janecki A, Jakubowiak A, Steinberger A. Effect of cadmium chloride on transepithelial electrical resistance of Sertoli cell monolayers in two-compartment cultures - a new model for toxicological investigations of the “blood-testis” barrier *in vitro*. Toxicol Appl Pharmacol 1992;112:51–57. [PubMed: 1733048]

Kamitani A, Yamada H, Kinuta M, Watanabe M, Li SMT, McNiven MA, Kumon H, Takei K. Distribution of dynamins in testis and their possible relation to spermatogenesis. Biochem Biophys Res Commun 2002;294:261–267. [PubMed: 12051704]

Katzmann DJ, Odorizzi G, Emr SD. Receptor downregulation and multivesicular-body sorting. Nat Rev Mol Cell Biol 2002;3:893–905. [PubMed: 12461556]

Le TL, Yap AS, Stow JL. Recycling of E-cadherin: A potential mechanism for regulating cadherin dynamics. J Cell Biol 1999;146:219–232. [PubMed: 10402472]

Lee NPY, Cheng CY. Regulation of Sertoli cell tight junction dynamics in the rat testis via the nitric oxide synthase/soluble guanylate cyclase/3′,5′-cyclic guanosine monophosphate/protein kinase G signaling pathway: an *in vitro* study. Endocrinology 2003;144:3114–3129. [PubMed: 12810568]

Lee NPY, Cheng CY. Protein kinases and adherens junction dynamics in the seminiferous epithelium of the rat testis. J Cell Physiol 2005;202:344–360. [PubMed: 15389520]

Lee NPY, Mruk DD, Conway AM, Cheng CY. Zyxin, axin, and Wiskott-Aldrich syndrome protein are adaptors that link the cadherin/catenin protein complex to the cytoskeleton at adherens junctions in the seminiferous epithelium of the rat testis. J Androl 2004;25:200–215. [PubMed: 14760006]

Li MWM, Xia W, Mruk DD, Wang CQF, Yan HHY, Siu MKY, Lui WY, Lee WM, Cheng CY. TNFα reversibly disrupts the blood-testis barrier and impairs Sertoli-germ cell adhesion in the seminiferous epithelium of adult rat testes. J Endocrinol 2006;190:313–329. [PubMed: 16899565]

Lie P, Xia W, Wang C, Mruk D, Yan H, Wong C, Lee W, Cheng C. Dynamin II interacts with the cadherin- and occludin-based protein complexes at the blood-testis barrier in adult rat testes. J Endocr 2006;191:571–586. [PubMed: 17170215]

Lui WY, Cheng CY. Regulation of cell junction dynamics by cytokines in the testis - a molecular and biochemical perspective. Cytokine & Growth Factor Rev 2007;18:299–311. [PubMed: 17521954]

Lui WY, Lee WM, Cheng CY. Transforming growth factor-β3 perturbs the inter-Sertoli tight junction permeability barrier *in vitro* possibly mediated via its effects on occludin, zonula occludens-1, and claudin-11. Endocrinology 2001;142:1865–1877. [PubMed: 11316752]

Lui WY, Lee WM, Cheng CY. Transforming growth factor-β3 regulates the dynamics of Sertoli cell tight junctions via the p38 mitogen-activated protein kinase pathway. Biol Reprod 2003a;68:1597–1612. [PubMed: 12606350]

Lui WY, Wong CH, Mruk DD, Cheng CY. TGF-β3 regulates the blood-testis barrier dynamics via the p38 mitogen activated protein (MAP) kinase pathway: an *in vivo* study. Endocrinology 2003b; 144:1139–1142. [PubMed: 12639893]

Massague J. TGFβ in cancer. Cell 2008;134:215–230. [PubMed: 18662538]

Massol P, Montcourrier P, Guillemot JC, Chavrier P. Fc receptor-mediated phagocytosis requires CDC42 and Rac1. EMBO J 1998;17:6219–6229. [PubMed: 9799231]

Maxfield FR, McGraw TE. Endocytic recycling. Nature Rev Mol Cell Biol 2004;5:121–132. [PubMed: 15040445]

McNiven MA, Cao H, Pitts KR, Yoon Y. The dynamin family of mechanoenzymes: pinching in new places. Trends Biochem Sci 2000;25:115–120. [PubMed: 10694881]

Meng J, Holdcraft RW, Shima JE, Griswold MD, Braun RE. Androgens regulate the permeability of the blood-testis barrier. Proc Natl Acad Sci USA 2005;102:16696–16670. [PubMed: 16275920]

Morimoto S, Nishimura N, Terai T, Manabe S, Yamamoto Y, Shinahara W, Miyake H, Tashiro S, Shimada M, Sasaki T. Rab13 mediates the continuous endocytic recycling of occludin to the cell surface. J Biol Chem 2005;280:2220–2228. [PubMed: 15528189]

Mruk DD, Cheng CY. Sertolin is a novel gene marker of cell-cell interactions in the rat testis. J Biol Chem 1999;274:27056–27068. [PubMed: 10480919]

Mruk DD, Cheng CY. Sertoli-Sertoli and Sertoli-germ cell interactions and their significance in germ cell movement in the seminiferous epithelium during spermatogenesis. Endocr Rev 2004;25:747–806. [PubMed: 15466940]

Pelletier R, Byers S. The blood-testis barrier and Sertoli cell junctions: structural considerations. Microsc Res Tech 1992;20:3–33. [PubMed: 1611148]

Piper RC, Luzio JP. Ubiquitin-dependent sorting of integral membrane proteins for degradationin lysosomes. Curr Opin Cell Biol 2007;19:459–465. [PubMed: 17689064]

Retta SF, Barry ST, Critchley DR, Defilippi P, Silengo L, Tarone G. Focal adhesion and stress fiber formation is regulated by tyrosine phosphatase activity. Exp Cell Res 1996;229:307–317. [PubMed: 8986614]

Russell L. Movement of spermatocytes from the basal to the adluminal compartment of the rat testis. Am J Anat 1977;148:313–328. [PubMed: 857632]

Setchell B, Waites G. Changes in the permeability of the testicular capillaries and of the “blood-testis barrier” after injection of cadmium chloride in the rat. J Endocrinol 1970;47:81–86. [PubMed: 5428920]

Sever S, Damke H, Schmid SL. Dynamin: GTP controls the formation of constricted coated pits, the rate limiting step in clathrin-mediated endocytosis. J Cell Biol 2000;150:1137–1147. [PubMed: 10974001]

Siu MKY, Cheng CY. Dynamic cross-talk between cells and the extracellular matrix in the testis. BioEssays 2004;26:978–992. [PubMed: 15351968]

Siu MKY, Lee WM, Cheng CY. The interplay of collagen IV, tumor necrosis factor-α, gelatinase B (matrix metalloprotease-9), and tissue inhibitor of metalloprotease-1 in the basal lamina regulates Sertoli cell-tight junction dynamics in the rat testis. Endocrinology 2003a;144:371–387. [PubMed: 12488366]

Siu MKY, Mruk DD, Lee WM, Cheng CY. Adhering junction dynamics in the testis are regulated by an interplay of β1-integrin and focal adhesion complex (FAC)-associated proteins. Endocrinology 2003b;144:2141–2163. [PubMed: 12697723]

Siu MKY, Wong CH, Lee WM, Cheng CY. Sertoli-germ cell anchoring junction dynamics in the tesis are regulated by an interplay of lipid and protein kinases. J Biol Chem 2005;280:25029–25047. [PubMed: 15870075]

Skinner, M. Secretion of growth factors and other regulatory factors. In: Russell, L.; Griswold, M., editors. The Sertoli Cell. Cache River Press; Clearwater: 1993. p. 237-247.

Walsh S, Hopkins A, Nusrat A. Modulation of tight junction structure and function by cytokines. Adv Drug Deliv Rev 2000;41:303–313. [PubMed: 10854688]

Wang RS, Yeh S, Chen LM, Lin HY, Zhang C, Ni J, Wu CC, di Sant’Agnese PA, deMesy-Bentley KL, Tzeng CR, Chang C. Androgen receptor in Sertoli cell is essential for germ cell nursery and junction complex formation in mouse testes. Endocrinology 2006;147:5624–5633. [PubMed: 16973730]

Wong CH, Mruk DD, Lui WY, Cheng CY. Regulation of blood-testis barrier dynamics: an *in vivo* study. J Cell Sci 2004;117:783–798. [PubMed: 14734653]

Wong EW, Mruk DD, Lee WM, Cheng CY. Par3/Par6 polarity complex coordinates apical ectoplasmic specialization and blood-testis barrier restructuring during spermatogenesis. Proc Natl Acad Sci U S A 2008a;105:9657–9662. [PubMed: 18621709]

Wong EWP, Mruk DD, Cheng CY. Biology and regulation of ectoplasmic specialization, an atypical adherens junction type, in the testis. Biochim Biophys Acta 2008b;1778:692–708. [PubMed: 18068662]

Xia W, Cheng CY. TGF-β3 regulates anchoring junction dynamics in the seminiferous epithelium of the rat testis via the Ras/ERK signaling pathway: An *in vivo* study. Dev Biol 2005;280:321–343. [PubMed: 15882576]

Xia W, Mruk DD, Lee WM, Cheng CY. Cytokines and junction restructuring during spermatogenesis - a lesson to learn from the testis. Cytokine Growth Factor Rev 2005;16:469–493. [PubMed: 16023885]

Xia W, Mruk DD, Lee WM, Cheng CY. Differential interactions between transforming growth factor-β3/TβR1, TAB1, and CD2AP disrupt blood-testis barrier and Sertoli-germ cell adhesion. J Biol Chem 2006;281:16799–16813. [PubMed: 16617054]

Yan HHY, Cheng CY. Laminin α3 forms a complex with β3 and γ3 chains that serves as the ligand for α6β1-integrin at the apical ectoplasmic specialization in adult rat testes. J Biol Chem 2006;281:17286–17303. [PubMed: 16608848]

Yan HHY, Mruk DD, Cheng CY. Junction restructuring and spermatogenesis: The biology, regulation, and implication in male contraceptive development. Curr Top Dev Biol 2007;80:57–92. [PubMed: 17950372]

Yan HHY, Mruk DD, Lee WM, Cheng CY. Blood-testis barrier dynamics are regulated by testosterone and cytokines via their differential effects on the kinetics of protein endocytosis and recycling in Sertoli cells. FASEB J 2008;22:1945–1959. [PubMed: 18192323]

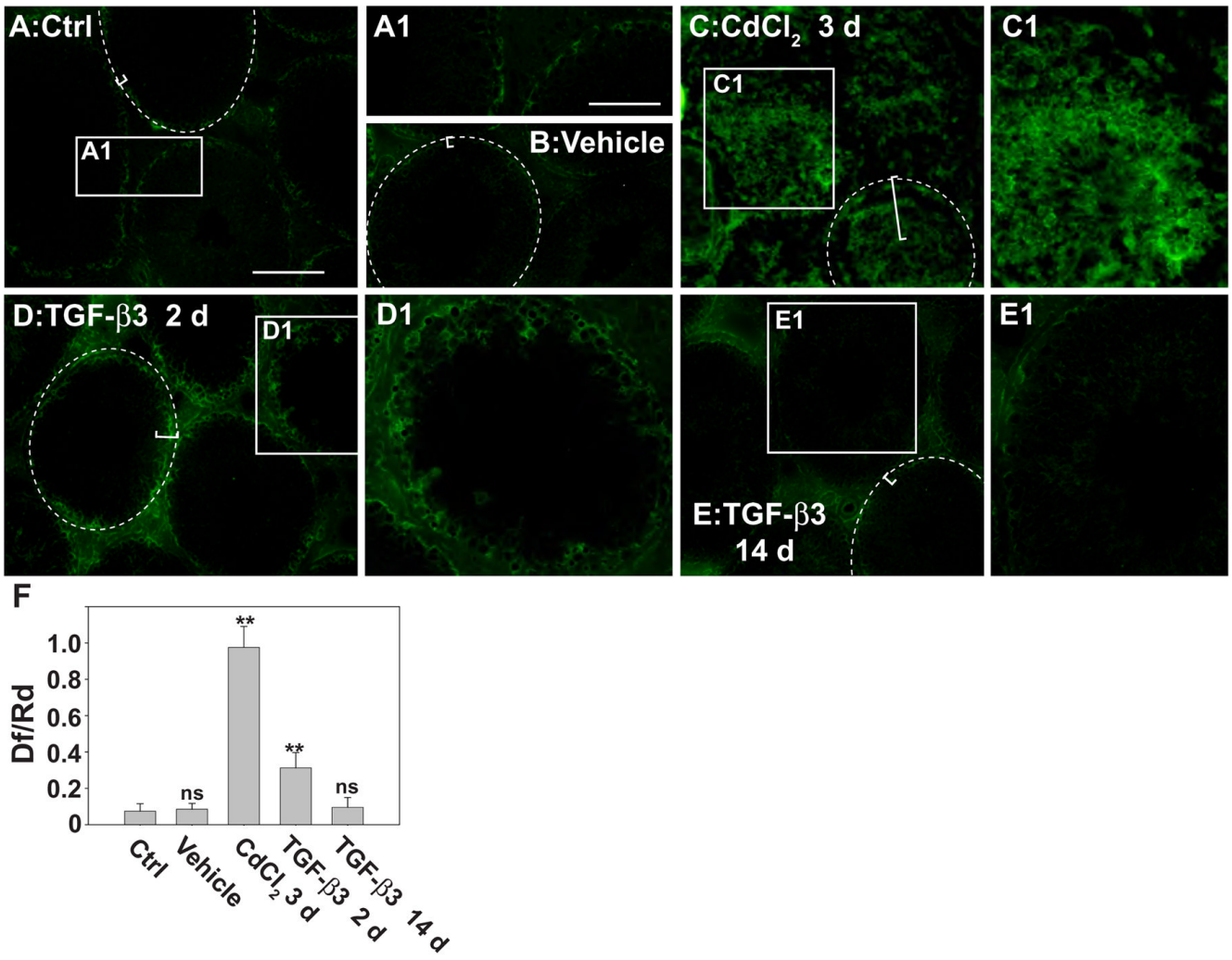

Figure 1. A study to examine the effects of TGF-β3 on the BTB integrity using an *in vivo* functional assay

As described in *Materials and Methods*, FITC (green fluorescence) was administered to rats via the jugular vein in controls [Ctrl, normal rats (A); and Vehicle, rats treated with saline (B); ~300 gm b.w.] on day 0, and at specified time points following treatments either with $CdCl_2$ at 3 mg/kg b.w., i.p. on day 3, positive control, which is known to disrupt the BTB integrity (C); with TGF-β3 at 200 ng/testis (intratesticular administration) on day 2 (D) or day 14 (E). About 90 min thereafter, rats were sacrificed by CO_2 asphyxiation, and the BTB integrity was assessed by its ability to restrict the diffusion of FITC across the barrier to enter the adluminal compartment of the seminiferous epithelium (the relative location of the BTB in the seminiferous epithelium near the basement membrane in a selected seminiferous tubule is annotated by the white circle in broken line, see A–E). The boxed area in A, C, D and E is magnified and shown in the corresponding A1, C1, D1 and E1. Bar in A is 60 μm, which applies to B, C, D and E; bar in A1 is 25 μm, which applies to C1, D1 and E1. In (F), this bar graph summarizes results on the distance traversed by the green fluorescence (FITC) from the BTB (Df) (see the white bracket in A, B, D and E) *vs.* the radius of the seminiferous tubule (see the white bracket in C) for different treatment groups vs. controls. For an oval-shaped tubule, the radius is estimated by the mean of the longer and the shorter radii. For each treatment group and controls, at least 3 rats were used. Each bar is the mean±SD of $n = 100$ tubules from three

rats that were randomly selected and measured. ns, not significantly different from Ctrl by ANOVA; **, $p<0.01$.

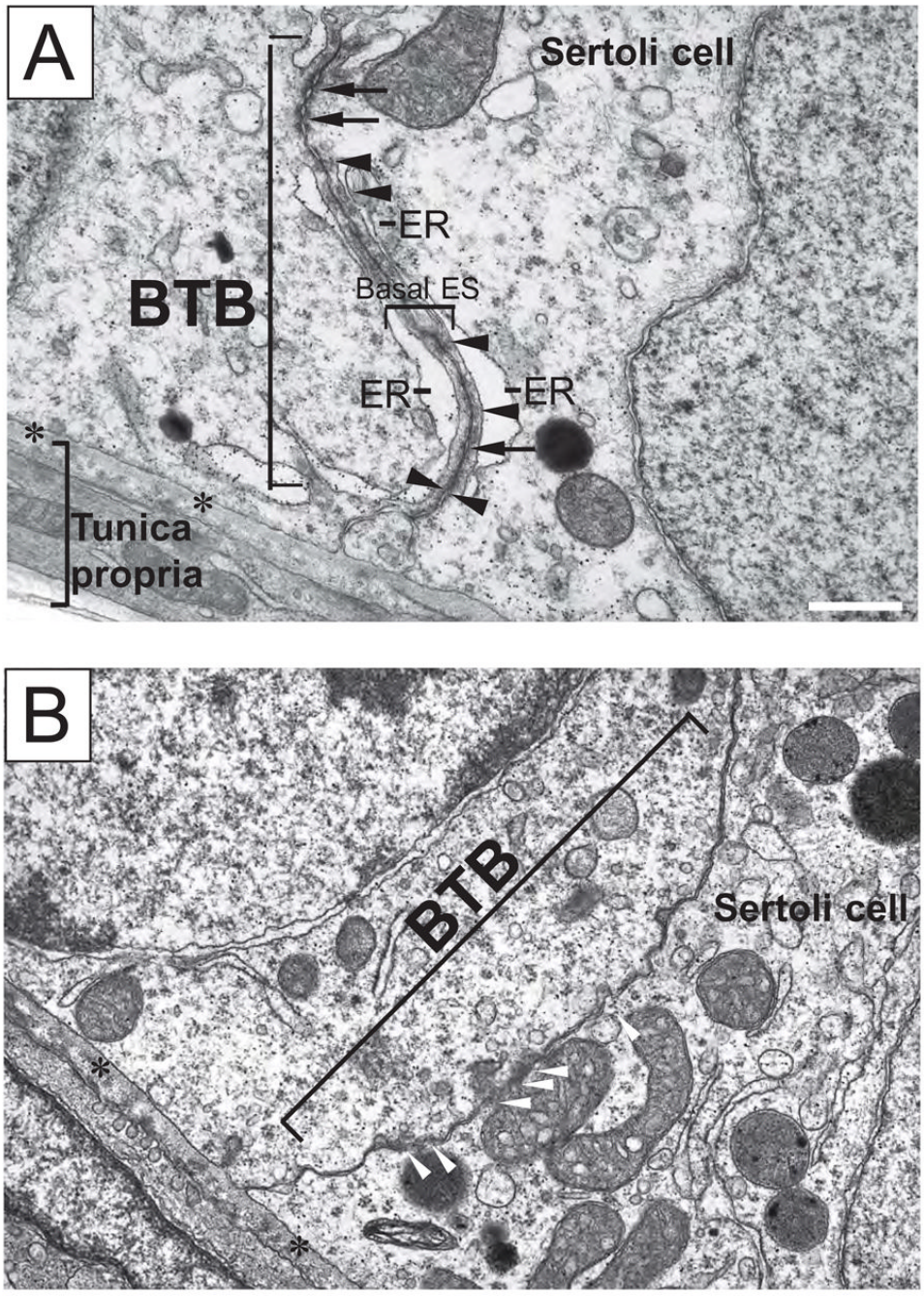

Figure 2. A study to assess TGF-β3-induced ultrastructural changes at the BTB in adult rat testes

Adult rats (~300 gm b.w.) were treated with a single dose of recombinant TGF-β3 on day 0 and terminated on day 2 (n = 2) *versus* rats treated with vehicle control or untreated normal rats. (A) This micrograph is the cross-section of a testis from a rat in the vehicle control group where two adjacent Sertoli cells created the BTB in the seminiferous epithelium were found, resting on the tunica propria (see asterisks, which represent the basement membrane). The BTB in this rat from the vehicle control group was similar to normal rat testes, which is typified by the presence of TJ (see the 'kisses' annotated by the black arrows) and the basal ES. The basal ES is defined by the actin filament bundles (see black arrowheads) sandwiched between the endoplasmic reticulum (ER) and the plasma membrane of the Sertoli cell (the two opposing

black arrows represent the two apposing Sertoli cell plasma membranes). (B) This is the cross-section of the testis from a rat treated with TGF-β3. The relative location of the BTB was bracketed here (see B *vs.* A) between two adjacent Sertoli cells in the seminiferous epithelium, however, no distinguishable basal ES (e.g., actin filament bundles, ER) or TJ ultrastructures were found, and visible damage was detected at the Sertoli-Sertoli cell interface (see white arrowheads). Bar in A = 0.5 μm, which applies to B.

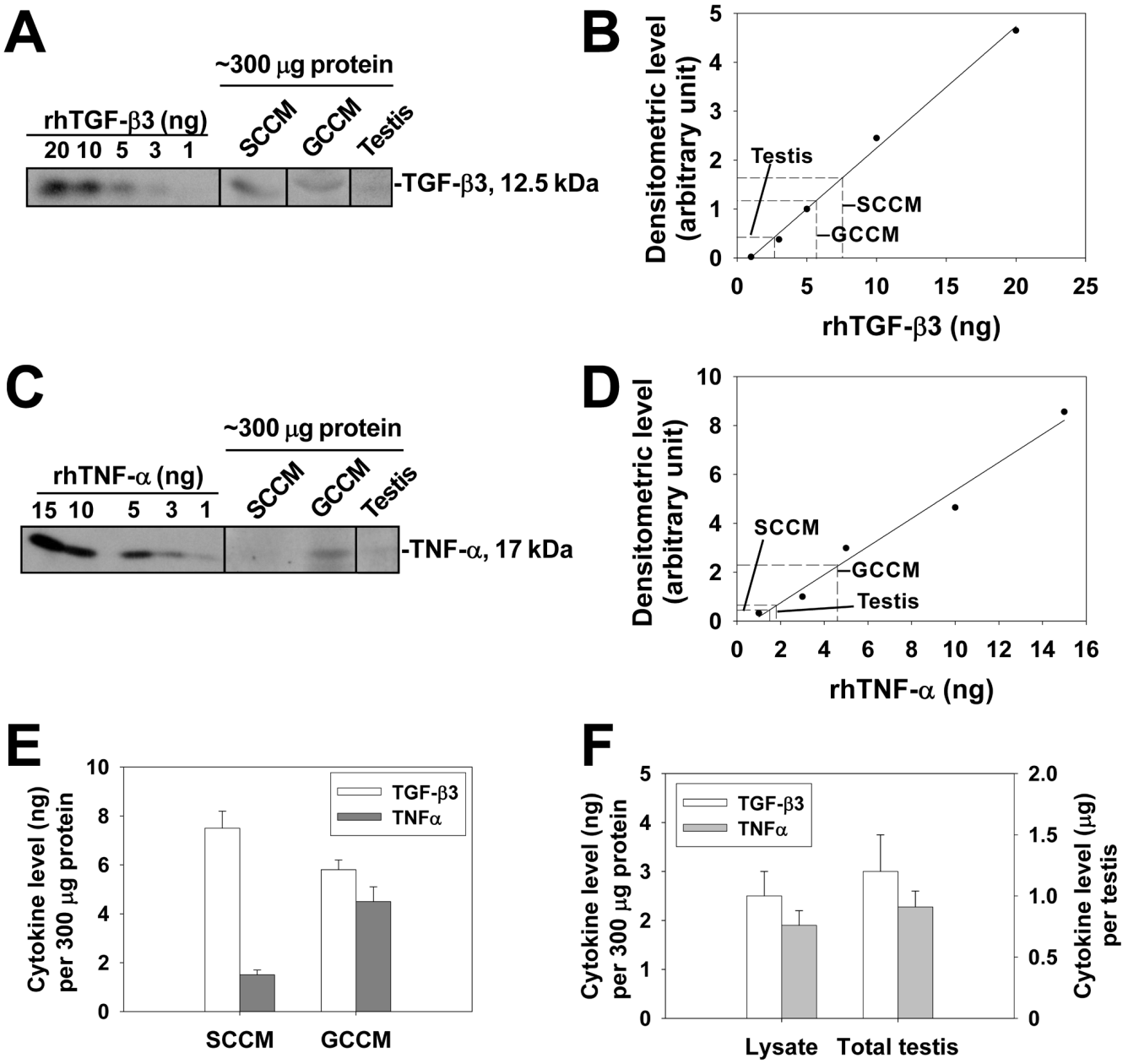

Figure 3. A study to estimate the relative levels of TGF-β3 and TNFα in SCCM and GCCM *versus* adult rat testes

Different concentrations of recombinant human TGF-β3 (rhTGF-β3) (A, B) and recombinant human TNFα (rhTNFα) (C, D) proteins were resolved by SDS-PAGE, and the relative levels of these cytokines in 300 μg protein of SCCM, GCCM and lysates of testes (testis) were estimated by interpolating the corresponding densitometric level against the standard (B, D) and compared (E, F). The levels of these cytokines in testes were also estimated and expressed as per testis content and shown in (F). Each bar is a mean ± SD of $n = 3$.

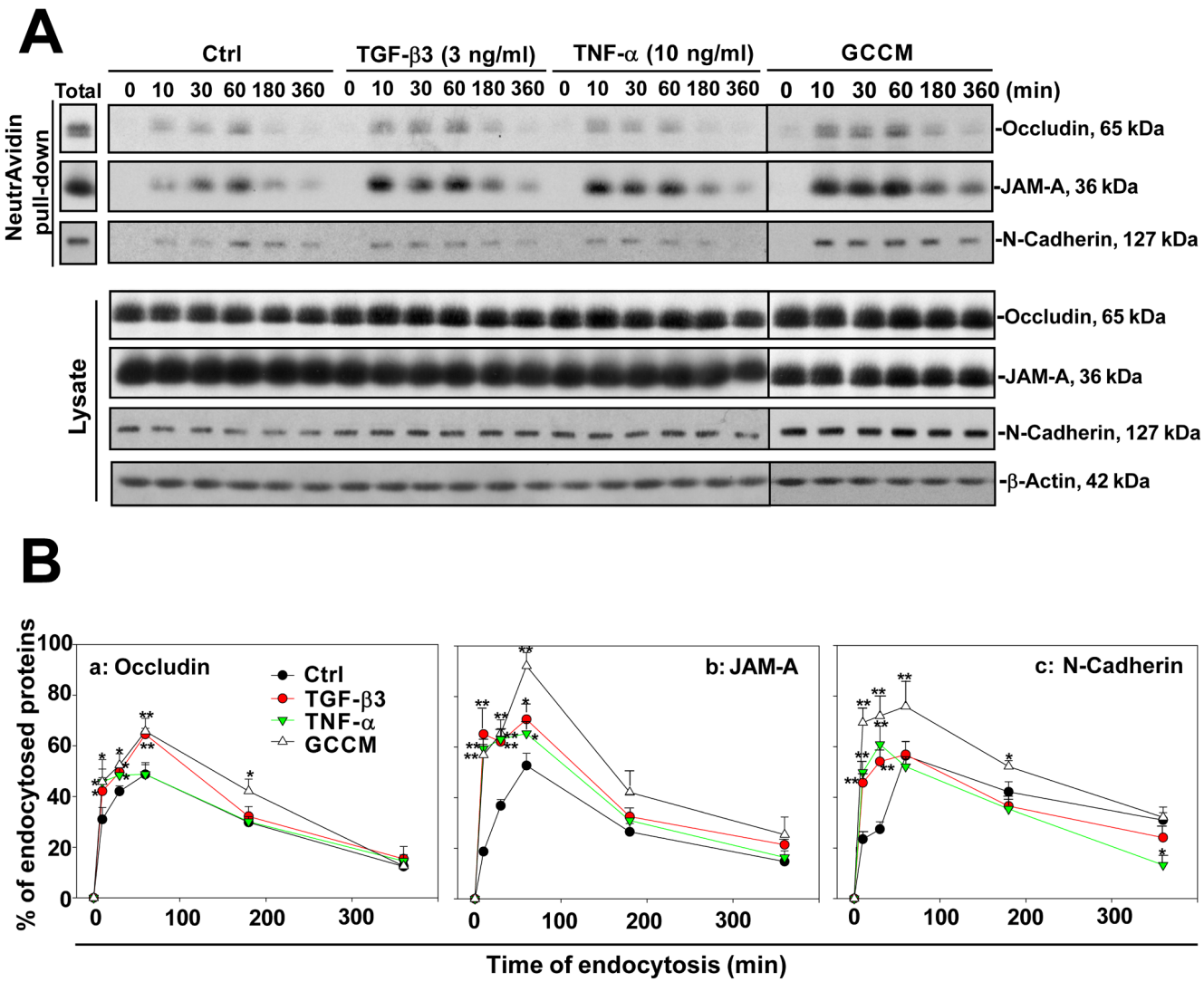

Figure 4. TGF-β3, TNFα and GCCM accelerate protein endocytosis at the BTB

The kinetics of internalization of integral membrane proteins at the BTB were assessed by using cell surface protein biotinylation, to be followed by tracking the appearance of biotinylated proteins in cell cytosol over time at 0, 10, 30, 60, 180 and 360 min, by immunoblotting with specific antibodies with Sertoli cell cultures as described in *Materials and methods*. (A) Immunoblot analyses of endocytosed occludin, JAM-A and N-cadherin in Sertoli cells harvested at different time points following cell surface biotinylation. Biotinylated cell surface proteins from Sertoli cells were allowed to undergo endocytosis at 35 °C without treatment (Ctrl), or treated with TGF-β3 (3 ng/ml), TNFα (10 ng/ml) or GCCM (~50 μg protein/ml). Non-internalized biotinylated cell surface proteins were stripped by a quenching buffer to remove the biotin, and the endocytosed proteins were pulled down by NeutrAvidin beads and analyzed by immunoblotting using the corresponding specific antibodies (see Table 1). Total = the amount of total biotinylated Sertoli cell surface proteins after the 30-min biotinylation without the biotin-stripping step at time 0. Cell lysates without NeutrAvidin-agarose-pull down were also analysed by immunoblotting (lower panel) to assess any changes in the steady-state protein levels following cytokine treatment during the experimental period. The kinetics of internalization of occludin, JAM-A and N-cadherin were summarized in

corresponding graphs in a, b and c shown in (B) by plotting the % of endocytosed protein *vs.* total biotinylated protein, [endocytosed and biotinylated protein/total biotinylated cell surface proteins] × 100%, (y-axis) against time (x-axis). Each data point is a mean ± SD of $n = 3$. *, $P<0.05$; **, $P<0.01$ by two-way ANOVA; other data points were not significant different from their corresponding controls. Abbreviations used in B:a are applicable to b and c.

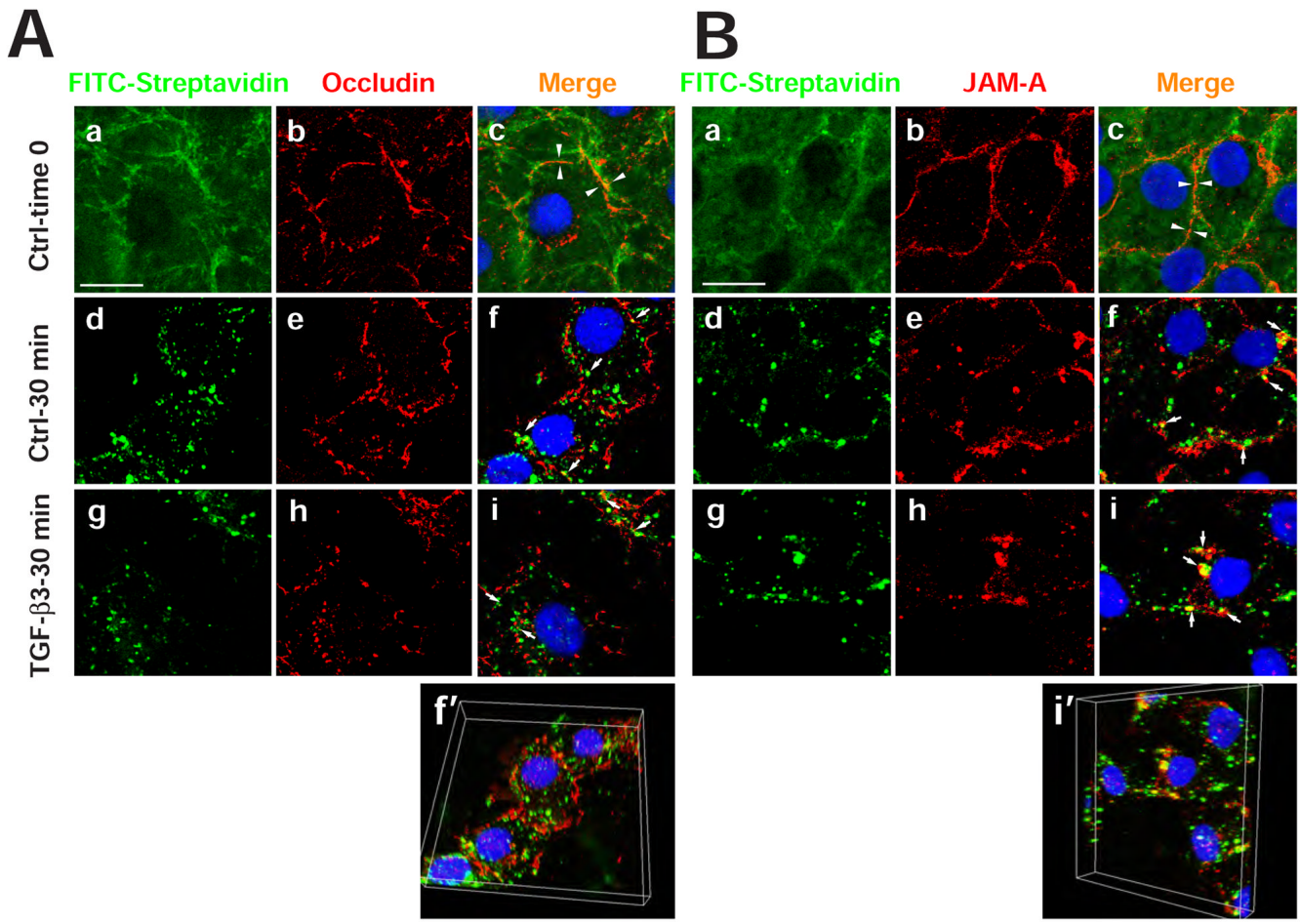

Figure 5. Confocal microscopy analysis of endocytosed (and biotinylated) proteins at the BTB using the *in vitro* Sertoli cell model following treatment with TGF-β3 *versus* controls

Fluorescent staining of occludin (red fluorescence, b, e, h) in (A) and JAM-A (red fluorescence, b, e, h) in (B) represented the cell surface biotinylated (b & e in A & B) protein at time 0 or both cell surface biotinylated *and* endocytosed biotinylated protein (e & h in A & B) *versus* total cell surface labeled biotinylated proteins visualized by FITC-streptavidin (green fluorescence, a, d, g for both panels) by confocal microscopy in Sertoli cell cultures without (Ctrl) and with treatment of TGF-β3 (3 ng/ml). Selected representative images from series of the z-stack slices were shown. At time 0 (A-a, b & c and B-a, b & c) biotinylated proteins were predominantly found at the cell-cell interface and cell surface in these primary Sertoli cell cultures. After 30 min incubation to allow endocytosis with (A-g, h & i; B-g, h & i) or without (A-d, e & f; B-d, e & f) TGF-β3 treatment (3 ng/ml), remaining biotin on the cell surface were quenched and the green fluorescence staining represents internalized biotinylated proteins, which appeared in punctate vesicles (C-d & g; D-d & g). Bar = 15 μm in C-a and D-a, which applies to all remaining micrographs. Apposing white arrowheads indicate intact junction protein fibrils (A-c & B-c); white arrows indicate endocytosed junction proteins (A-f, i & B-f, i). The f' and i' under Panels A and B illustrate the representative micrographs of the corresponding 3-dimensional projections of f and i shown in Panels A and B illustrating changes in integral membrane protein (e.g., JAM-A in i') distribution following TGF-β3 treatment by 30 min at the time of cytokine-induced BTB disruption in these cultures. These images were reconstructed from a series of confocal images (z-stack) using Imaris software (Version 5.0, Bitplane Inc., St Paul, MN). The corresponding antibodies and their working

dilution used for the experiments reported herein are found in Table 1. These micrographs are representative results of a single experiment, which was repeated two more times using different batches of cell cultures and yielded similar results.

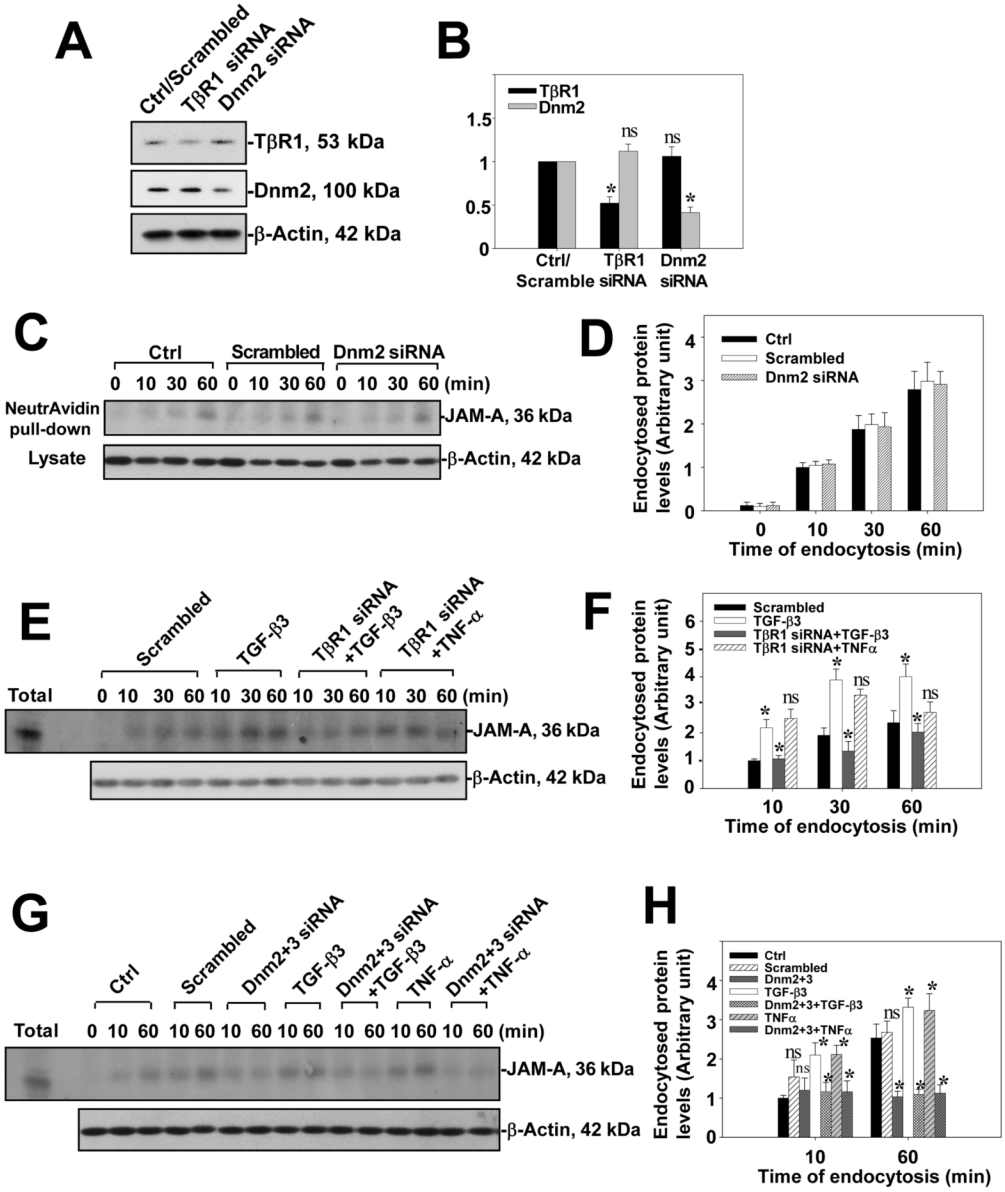

Figure 6. Silencing of TβR1 or dynamins by specific siRNA duplexes perturbs TGF-β3-enhanced protein endocytosis at the BTB

Sertoli cells were cultured and transfected with corresponding specific siRNA duplexes, to be followed by endocytosis assay and immunblot analysis to quantify protein internalization. (A–B) Knockdown of TGF-β receptor 1 (TβR1) and dynamin2 (Dnm2) using specific siRNA duplex *vs.* Ctrl (i.e., scrambled Ctrl siRNA) duplex in Sertoli cells (see Table 2). In (A), these are immunoblots using Sertoli cell lysates immunostained for corresponding target proteins of TβR1 and Dnm2, wherein β-actin served as protein loading control. (B) The steady-state level of target protein in Sertoli cells transfected with Ctrl/Scrambled siRNA duplex was arbitrary set at 1 against which different treatment groups were compared by ANOVA to be followed by the Dunnett's test. *, $p<0.01$; ns, not significantly different. (C–D) Knockdown of dynamin 2 *alone* did not affect endocytosis of JAM-A as illustrated in this endocytosis experiment (C) and the composite results of 3 experiments shown in (D). (E–F) Knockdown of TβR1 abolished TGF-β3-induced accelerated internalization of JAM-A but not those induced by TNFα.

Statistical analysis was performed by comparing (i) Scrambled *vs.* TGF-β3, (ii) TGF-β3 *vs.* TβR1 siRNA+TGF-β3, and (iii) TGF-β3 *vs.* TβR1 siRNA+TNFα at 10-, 30- and 60-min following endocytosis by ANOVA to be followed by the Dunnett's test; ns, not significantly different; *, $p<0.01$. (G-H) Knockdown of *both* dynamins 2 and 3 abolished the cytokine-induced accelerated internalization of JAM-A. Each bar graph shown in B, D, F and H is the mean±SD of 3 experiments. Statistical analysis was performed by comparing (i) Ctrl (i.e., Sertoli cells without subject to transfection with any siRNA duplex) *vs.* Scrambled, (ii) Ctrl *vs.* Dnm2+3, (iii) Ctrl *vs.* TGF-β3, (iv) TGF-β3 *vs.* Dnm2+3+TGF-β3, (v) Ctrl *vs.* TNFα, (vi) TNFα vs. Dnm2+3+TNFα at 10- and 60-min following endocytosis by ANOVA to be followed by the Dunnett's test; ns, not significantly different; *, $p<0.01$.

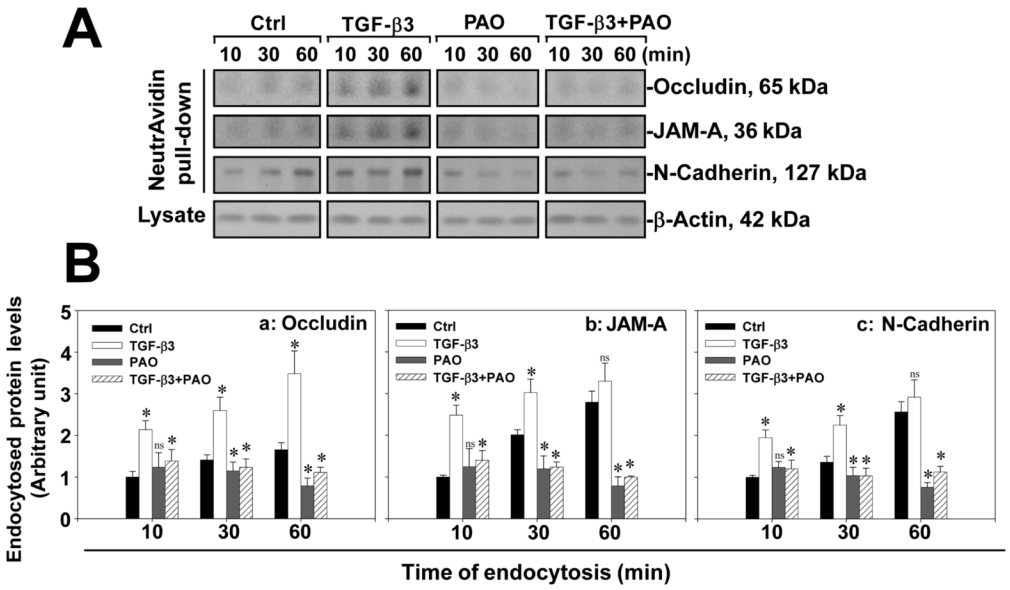

Figure 7. PAO inhibits endogenous protein endocytosis as well as TGF-β3-induced enhancement of protein endocytosis at the BTB

(A–B) PAO, a specific inhibitor of clathrin, was shown to block the clathrin-mediated endocytosis of occludin, JAM-A and N-cadherin in Sertoli cells cultured *in vitro* with functional BTB. β-Actin serves a protein loading control illustrating the same amount of protein (~400 μg per sample) was used for this analysis. Pretreatment of Sertoli cells when functional BTB on day 4 with PAO at 10 μM for 30 min prior to endocytosis assays as described in *Materials and Methods* was shown to abolish the endogenous protein endocytosis (see panel 3 *vs.* panel 1 in A) as well as TGF-β3-induced acceleration of protein endocytosis (see panel 4 *vs.* panel 2 in A), see also B. Each bar graph in B is the mean±SD of 3 experiments, and each experiment had duplicate cultures. Statistical analysis was performed by comparing (i) Ctrl *vs.* TGF-β3, (ii) Ctrl *vs.* PAO, and (iii) TGF-β3 *vs.* TGF-β3+PAO at 10-, 30- and 60-min following endocytosis by ANOVA to be followed by the Dunnett's test; ns, not significantly different; *, $p<0.01$.

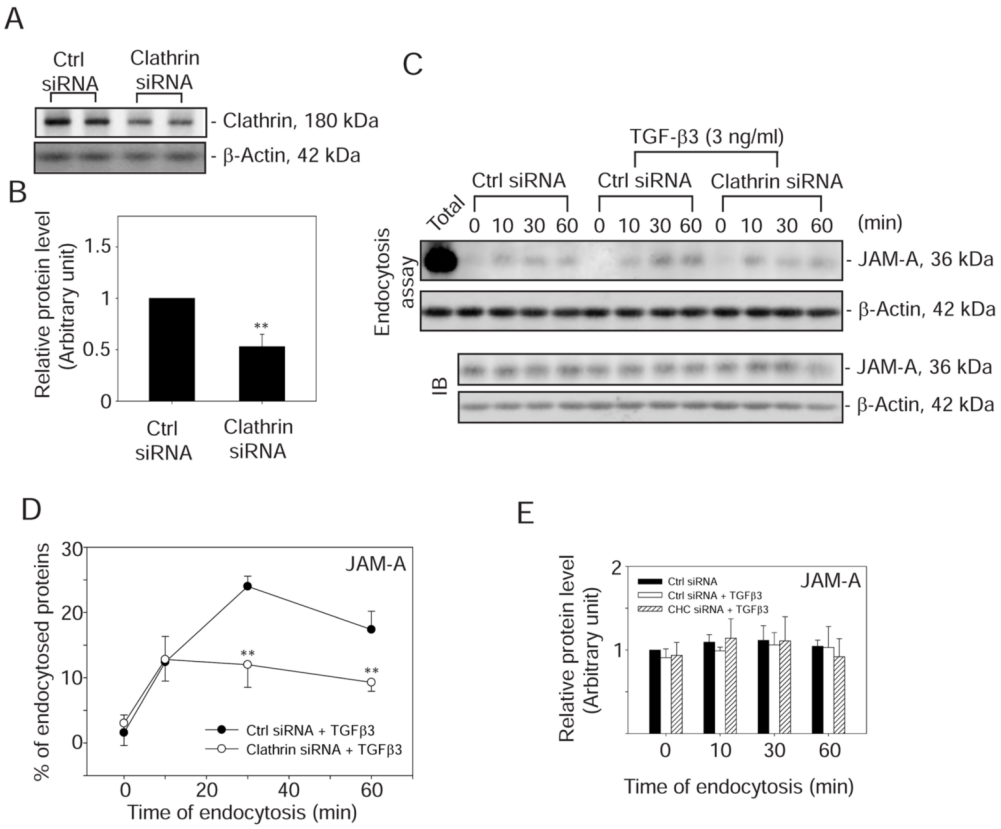

Figure 8. A study to assess the effects of knockdown of clathrin heavy chain by RNAi on the TGF-β3-enhanced protein endocytosis at the BTB

(A) Two days following isolation, Sertoli cells were transfected with specific siRNA duplexes against clathrin heavy chain (Clathrin siRNA) or non-targeting control siRNA (Ctrl siRNA) (see *Materials and Methods*). Cells (in two replicates, ~80 μg protein per lane, top panel) were harvested 2 days thereafter to assess the steady-state protein level of clathrin heavy chain protein by immunoblotting. β-Actin serves as the protein loading control. (B) Composite result from three independent experiments was shown where clathrin heavy chain protein level was normalized against loading control β-actin. Protein level of cells transfected with non-targeting control was arbitrarily set at 1. Data are mean ± SD of $n = 3$. (C) Sertoli cells as indicated in (A) on Day 2 after RNAi *vs.* controls were used for biotinylation, following quenching to remove unlabeled cell surface biotin (see *Materials and Methods*). Endocytosis assay was performed in the absence or presence of TGF-β3 (3 ng/ml) and incubated at 35 °C to allow protein internalization to occur and terminated at 0, 10, 30 and 60 min (see the two Top Panels). Cells lysate were harvested and biotinylated proteins were pulled down by NeutrAvidin beads. β-Actin was used as loading control to ensure equal amount of protein was used for the pull-down assay. Cell lysates alone (without pull-down) were used obtained in parallel experiment to probe for JAM-A by immunoblotting (IB) to examine if the silencing of clathrin heavy chain would affect the JAM-A steady-state protein level. (D) Percentage of endocytosed proteins *vs.* total biotinylated surface protein were plotted against time. Results from three independent experiments were shown where silencing of clathrin heavy chain resulted in an inhibition of TGF-β3-mediated protein endocytosis when compared to Ctrl siRNA. Each time point is mean ± SD of $n = 3$. (E) No significant difference in the steady-state protein levels of JAM-A in Sertoli cells was detected following silencing of clathrin heavy chain. Each bar is a mean ± SD of $n = 3$. **, $p < 0.01$ by one-way ANOVA followed by the Dunnett's test.

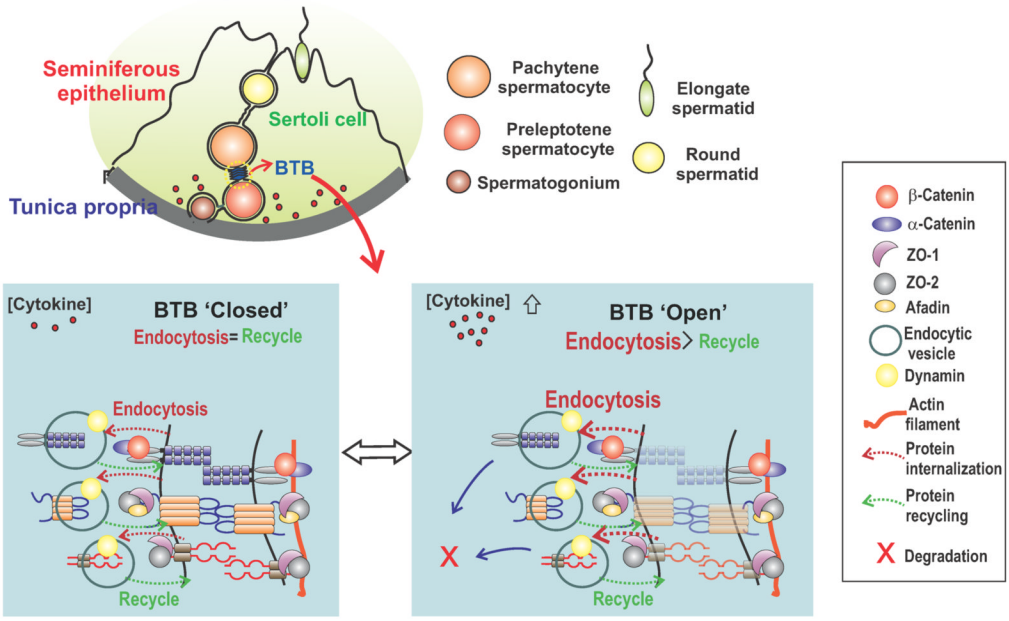

Figure 9. A schematic drawing to summarize the role of cytokines on BTB dynamics by regulating the kinetics of protein endocytosis at the BTB

Based on the results reported herein, we speculate that the status of the BTB, such as its 'opening' (right panel) or 'closing' (left panel), is largely dependent on the equilibrium between 'protein endocytosis' and 'protein recycling' at the BTB. During the seminiferous epithelium cycle at stages other than VIII–IX when the BTB remains 'closed', it is likely that the rate of protein endocytosis is equivalent or less than protein recycling (left panel); however at stages VIII–IX when preleptotene/leptotene spermatocytes are in transit to traverse the BTB, an elevated level of cytokines (e.g., TGF-β3, TNFα) enhances protein endocytosis, making the kinetics of protein endocytosis out pacing protein recycling, destabilizing the BTB integrity to facilitate spermatocyte migration (right panel).

Table 1

Primary antibodies used for different experiments in this report

Vendor	Target protein	Animal source*	Catalog #	Lot #	Usage**	Working dilution
Santa Cruz Biotechnology (Santa Cruz, CA):	**N-Cadherin**	Rabbit	sc-7939	J2105	IB	1:200
	TβR1	Rabbit	sc-398	E0305	IB	1:200
	β-Actin	Goat	sc-1616	D052	IB	1:1000
Invitrogen [Zymed Laboratories Inc., South San Francisco, CA)]:	**Occludin**	Rabbit	71–1500	51202542	IB	1:200
					IF	1:100
	JAM-A	Rabbit	36–1700	50393637	IB	1:250
					IF	1:100
BD Transduction Laboratories (San Diego, CA):	**Dynamin2**	Mouse	610245	0000085934	IB	1:1000
	Clathrin heavy chain	Mouse	610499	76274	IB	1:1000

* Rabbit or goat—polyclonal antibodies prepared in corresponding host animals; mouse—monoclonal antibodies. These antibodies cross-reacted with the corresponding target proteins in rats.

** IB: immunoblotting; IF: immunofluorescent microscopy

Table 2

Sequence of siRNA used in this study.

Gene		Sequence
Dnm2	Sense	5′-CCUCAAAAUACGGGAUGUGtt-3′
	antisense	5′-CACAUCCCGUAUUUUGAGGtt-3′
Dnm3	Sense	5′-GGCUUAAUAUGUUGUAUUGtt-3′
	antisense	5′-CAAUACAACAUAUUAAGCCtc-3′
Tgfbr1	Sense	5′-GGCAGAGAUUUAUCAGACUtt-3′
	antisense	5′-AGUCUGAUAAAUCUCUGCCtc-3′